AJO-DO

# Improving interproximal surface reconstruction via artificial intelligence–based tooth segmentation with crown-root integrated models: A preliminary study

**Amir Salloum,[a] Nabil Ghosn,[a,b] Alain Tauk,[a,b,c] Roland Kmeid,[a,c] and Joseph Bouserhal[d]**
*Beirut, Lebanon, and Boston, Mass*

**Introduction:** Tooth segmentation plays a fundamental role in digital diagnosis and design. The interproximal surface, a key area for accurate tooth segmentation, remains poorly captured due to intraoral scanner (IOS) limitations. The objective of this study was to evaluate the 3-dimensional accuracy of the interproximal surface in a dentition model segmented using the following: (1) IOS alone; (2) artificial intelligence (AI)–based IOS and cone-beam computed tomography (CBCT) fusion; and (3) IOS-CBCT fusion followed by manual interproximal adjustment. **Methods:** Fourteen extracted maxillary teeth were scanned by IOS to be used as a reference, then arranged in a full-arch configuration with moderate crowding. IOS and CBCT segmentation of the model and subsequent fusion of segmented crowns and roots were performed on the Relu AI-based platform (March 2022 version; Relu BV, Leuven, Belgium). The fused models were then manually adjusted at the interproximal surface, as seen from the axial CBCT slices. Three-dimensional deviation analyses were carried out on the 3 segmented models for the interproximal, outer, and total crown surfaces. Statistical analysis was conducted using repeated-measures analysis of variance, Friedman, Tukey honest significant difference, and Wilcoxon signed rank tests ($P < 0.05$). **Results:** Descriptive statistics revealed a tendency for IOS models to overestimate the interproximal surface compared with fused models. The manually adjusted models demonstrated significantly improved interproximal accuracy ($P < 0.05$). The total surface accuracy of fused models was significantly improved from IOS models ($P < 0.05$). Outer surface deviations did not vary. **Conclusions:** The preliminary findings suggest that CBCT integration significantly enhances the total surface accuracy of AI-segmented tooth models, whereas localized manual refinement further improves interproximal trueness. (Am J Orthod Dentofacial Orthop 2026;169:682-92)

Tooth segmentation, which involves separating individual teeth from the digital dentition model, is used in many digital dental applications, such as orthodontics, prosthetic dentistry, and digital implantology, to ensure predictable treatment planning and facilitate accurate simulation of clinical scenarios.[1–3] Little attention has been given to the adequate reproduction of the interproximal surface in studies evaluating tooth segmentation techniques, primarily because of the failure of the intraoral scanner (IOS) to capture it.[4–7] In evaluating multimodal cone-beam computed tomography–IOS (CBCT-IOS) reconstructions, studies, such as that of Qian et al,[8] have successfully addressed the occlusal problem, whereby occlusal surfaces of tooth crowns in CBCT scans were replaced with those of IOS crowns. However, the interproximal problem remains unsolved.

[a]Imaging Unit, Craniofacial Research Laboratory, Faculty of Dental Medicine, Saint-Joseph University of Beirut, Beirut, Lebanon;
[b]Department of Digital Dentistry, Faculty of Dental Medicine, Saint-Joseph University of Beirut, Beirut, Lebanon;
[c]Department of Orthodontics, Faculty of Dental Medicine, Saint-Joseph University of Beirut, Beirut, Lebanon;
[d]Department of Orthodontics, Henry M Goldman School of Dental Medicine, Boston, Mass

All authors have completed and submitted the ICMJE Form for Disclosure of Potential Conflicts of Interest, and none were reported.
This research did not receive any specific grant from funding agencies in the public, commercial, or not-for-profit sectors.
The ethics committee of Saint-Joseph University of Beirut has reviewed and approved the protocol of this study.

Address correspondence to: Amir Salloum, Imaging Unit, Craniofacial Research Laboratory, Faculty of Dental Medicine, Saint-Joseph University of Beirut, Beirut, Lebanon; e-mail, amir.salloum@net.usj.edu.lb.

Submitted, June 2025; revised and accepted, November 2025.
0889-5406/$36.00



https://doi.org/10.1016/j.ajodo.2025.11.025

IOS does not provide an accurate picture of the interproximal surface between teeth, whereby, as the interproximal distance decreases, the accuracy of the impression decreases.[9] This often produces a bridging effect, whereby teeth appear as 1 block because areas inaccessible by the scanner are connected based on outer surface data. The effect of this complication on tooth segmentation has been interpreted in the literature as variations in dental arch length[10] and inaccurate mesiodistal widths of segmented teeth.[11]

The emergence of deep learning (DL) has allowed fully automatic instance segmentation using software algorithms that are both accurate and efficient.[12–14] Im et al[15] studied the accuracy of traditional segmentation methods compared with DL-based models, concluding a comparable accuracy between landmark-based and DL-based methods. With insufficient interproximal information, automatic segmentation relies on the reconstruction of the interproximal surface based on training data. For instance, Kim et al[16] used general adversarial networks as a method of image completion to reconstruct the interdental areas of teeth scanned directly with an IOS. Such missing data have later led to numerous studies evaluating the validity of fully automatic tooth segmentation as opposed to manual, time-consuming methods.[17] Many of these studies point to an overestimation of tooth size from IOS segmentation alone. In particular, Yacout et al[11] suggest that both DL-based software packages and manual correction are unable to reproduce proximal anatomy.

In light of the novel concepts of multimodal fusion and artificial intelligence (AI)–based segmentation, the question arises as to whether multimodal reconstructions can accurately restore the interproximal surface. The primary objective of this study was to evaluate the 3-dimensional (3D) interproximal surface deviation among 3 segmented tooth models: IOS-derived, IOS-CBCT fused, and IOS-CBCT fused-adjusted. Therefore, teeth were segmented using IOS alone, then CBCT roots were automatically fused to IOS crowns to produce fused models, which were then adjusted at the interproximal surfaces using the CBCT slices at that level to obtain the fused-adjusted models. As a secondary objective, the total crown surface deviation is analyzed to determine the impact of interproximal inaccuracy on overall tooth crown reconstructions. Although the International Organization for Standardization (ISO) 5727 standard defines accuracy for a series of repeated measurements as the combination of trueness and precision, the objective of this study compels us to use the definition of accuracy applied in engineering and metrology studies, which would correspond to the ISO 5725 standard for trueness.[18] Therefore, for the objectives covered in this study, accuracy is defined as the closeness of a measured value to the true value.

## MATERIAL AND METHODS

Fourteen dry teeth were obtained from patients whose treatment plan included the extraction of 1 or more teeth. The anterior maxillary teeth (teeth 14 to 24) were acquired from 1 patient undergoing immediate guided implant therapy. A maxillary model of the same patient was obtained after jaw segmentation using CBCT. The remaining teeth were collected from other patients requiring extractions for orthodontic or strategic reasons. Written consent was obtained for the use of the extracted teeth and the maxillary model.

The selection criteria were permanent teeth with intact enamel, without any visible fractures, developmental defects, caries, or physical damage because of extraction.

All teeth were rinsed with normal saline and stored in prelabeled containers. Freshly extracted teeth were stored in distilled water at 37°C until use. Once model preparation began, the teeth were sterilized in an autoclave set to 121°C, 15 psi for 15 minutes to avoid cross-contamination.[19]

Figure 1 illustrates the steps followed for model preparation. The 14 teeth, held in place with pink modeling wax, were individually scanned with the Medit i700 (Medit, Seoul, South Korea) IOS to obtain reference models that would be considered ground truth for subsequent deviation analyses (Fig 1, *A*). The apices inserted into the wax were then scanned by turning the teeth over and trimming the wax base from the initial scan.

The teeth were aligned according to a predetermined configuration (Fig 1, *B*), and space analysis was conducted using Blenderfordental version 3.6 software (Blenderfordental Pty, Robina, Queensland, Australia) to verify that moderate anterior crowding did not exceed 4 mm. Using the same software, the segmented maxillary model was hollowed out, offset was applied, and a trabecular pattern was inserted inside the model using a Boolean operation to reproduce interior bone architecture (Fig 1, *C*). The aligned teeth were digitally placed over the model, and sockets were created to allow physical tooth insertion inside the model (Fig 1, *D*). A 2 mm bone-to-cementoenamel junction distance was adopted.

The alveolar bone model was then 3D-printed using dental model resin (Voco GmbH, Cuxhaven, Germany). A light body impression material (Imflex; Metabiomed, Korea), simulating trabecular bone in radiopacity, was poured into the printed model and the sockets of the teeth that were immediately inserted after (Fig 1, *E*). Pink modeling wax was added to simulate the gum and papillae.

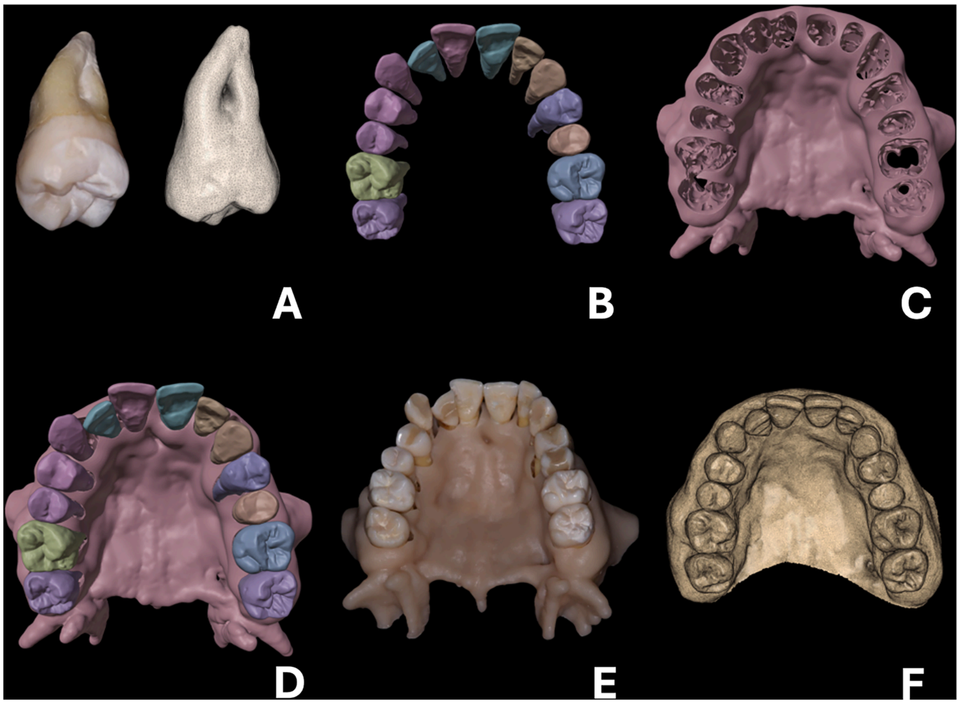


**Fig 1.** Model preparation: **A,** Individual tooth and its corresponding surface scan; **B,** Scanned teeth setup with moderate anterior crowding; **C,** Digital preparation of maxillary model with teeth sockets; **D,** Full digital model of scanned teeth aligned on the virtual maxillary bone model; **E,** Printed model with the teeth inserted in the sockets; **F,** Surface scan printed model after insertion of teeth and application of wax layer.

The study model was scanned with the Medit i700 (Medit) IOS, following the recommended procedure to simulate the clinical scenario (Fig 1, *F*).

Using a proper support, made of a styrofoam base and placed at the center of the area in which the patient's head would be positioned, a CBCT scan of the study model was acquired using the NewTom VGi (NewTom, Verona, Italy) CBCT unit, with the following technical specifications: field of view 120 mm $\times$ 120 mm, voxel size 0.15 $\times$ 0.15 $\times$ 0.15 $mm^3$, tube voltage 85 kV, tube current 10 mA, and frequency 85 kHz.

For the first technique (technique 1) involving IOS AI-based segmentation, the polygon file format file of the IOS model was uploaded to the Relu Virtual Patient Creator platform (March 2022 version; Relu BV, Leuven, Belgium), in which the teeth were automatically segmented using the software's algorithm (Fig 2, *A*).

For the second technique (technique 2), both IOS and CBCT scans were uploaded to the platform. An AI-automated registration, segmentation, and fusion of the IOS and CBCT scans took place, merging the IOS crown segmentation and CBCT root segmentation into individual fused teeth models (Fig 2, *B*).

For the third technique (technique 3), the obtained fused models from the Relu platform (Relu BV), aligned to the initially uploaded CBCT and IOS models, were imported into Blue Sky Plan software (version 4.12.13; Blue Sky Bio, Ill). The panoramic curve is drawn across the set of teeth to produce axial slices at the level of contact between adjacent teeth. The outlines of the segmented and fused teeth were then manually adjusted by a single operator, using the move outlines option (Fig 2, *C*). This process involved selecting each tooth individually and adjusting its segmented crown outline at the level of the interproximal surface as it appears in the axial and tangential CBCT slices. The slice-by-slice adjustment is done 1 tooth at a time by selecting the outline of the crown to be adjusted. Any gap or overlap near the area of contact between adjacent teeth is eliminated by adjusting the outline of the segmented crown. The 3 segmentation techniques are illustrated in Figure 2.

The present step involved selecting the interproximal surfaces of the tooth to be analyzed, as well as the outer and total surfaces. These regions of interest were compared across the 3 models to evaluate segmentation accuracy.

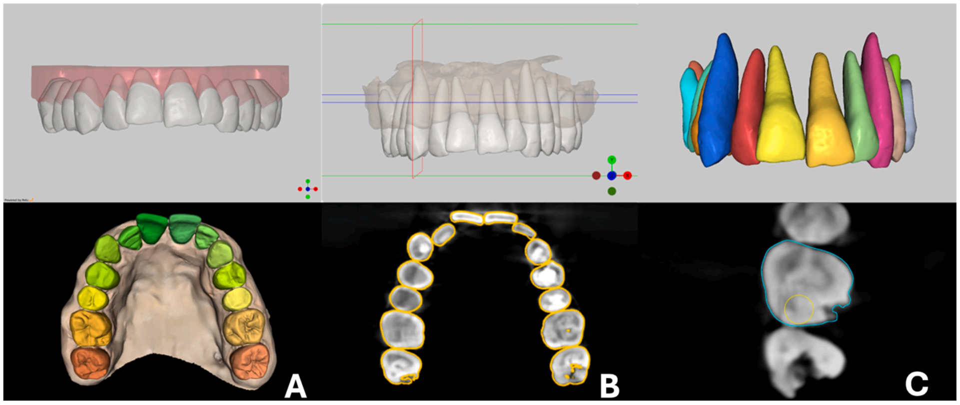


**Fig 2.** Segmentation techniques: **A,** IOS scan (*top*) and subsequent segmentation (*bottom*) using the Relu platform (Relu BV); **B,** CBCT and IOS segmentation fusion (*top*) with corresponding axial view from the CBCT scan (*bottom*); **C,** Fused models uploaded to Blue Sky Plan (Blue Sky Bio) (*top*) followed by contour modification (*bottom*) using the move outlines option (*yellow*) to obtain the fused-adjusted models.

A standardized method for the selection of the interproximal surface was adopted to exclude the outer crown surface not involved in the interdental contact. The Relu software (Relu BV) uses an AI-based completion algorithm to regenerate surfaces deemed inaccessible by the scanner head. These regions are geometrically defined by the software's algorithm during segmentation and remain open. These open crowns, which exhibit cutout interproximal surfaces, are closed off using the software's AI algorithm, yielding closed crowns. The reference tooth model was uploaded to Autodesk Meshmixer (Autodesk Inc, San Rafael, Calif), and superimposition with the open crowns allowed the selection and separation of the interproximal surfaces. The regions of the crown, excluding the interproximal surfaces, were defined as the outer surfaces. The union of both interproximal and outer surfaces is the total crown surface.

Because the interproximal surface is relatively small compared with the total surface, we anticipated a subsequent step to ensure the stability of root mean square (RMS) values: the separation of the interproximal surface from the total surface. The segmented model of each technique is superimposed over the reference model. Using Blenderfordental (B4D, Blenderfordental 2019), a Boolean operation was used to replicate the chosen interproximal surfaces of the reference models from the previous step on each of the 3 segmented models (Fig 3, *A-C*). This operation yielded 3 interproximal regions, corresponding to techniques 1, 2, and 3, that correspond identically to the interproximal region initially selected in the reference model (Fig 3, *D*).

Only 1 interproximal surface exists for the maxillary right and left second molars, yielding 26 interproximal surfaces, 14 total surfaces, and 14 outer surfaces to be compared with the reference scanned teeth by simple superimposition.

The IOS, fused, and fused-adjusted models, along with the total and outer surfaces of the reference model and the individual interproximal surfaces for each of the mentioned 4 models, were imported into the Medit Link (Medit) software for deviation analysis.

For the comparisons, a reference group and a target group were selected. The reference group corresponded to the given surface from the reference model to be compared, and the target group corresponded to 1 of the 3 segmented tooth models. After reference-target superimposition, a heat map illustrating 3D deviation was generated, and RMS error was collected for statistical analysis of the outer, interproximal, and total surfaces. For descriptive statistics of the interproximal area in particular, the average deviation (avg), plus average (avg +), minus average (avg –), and absolute average deviation (abs avg) were collected. These values indicate how much the volume of the segmented crowns is larger (avg +) or smaller (avg –) than the reference crown models for the same selected interproximal surface, as well as the overall negative or positive deviation (avg). The absolute values of the deviations are used to reflect the magnitude of error regardless of direction (abs avg). This was done for the purpose of determining whether teeth were being overestimated or underestimated in mesiodistal width at the level of the interproximal surface.

As illustrated in Figure 4, the various tooth models were visualized in 2 ways: 3D deviation analysis, yielding an RMS value for each studied surface and curvature display, yielding a topographical map of the tooth surface. To eliminate possible discrepancies at the level of the crown-root boundary and compensate

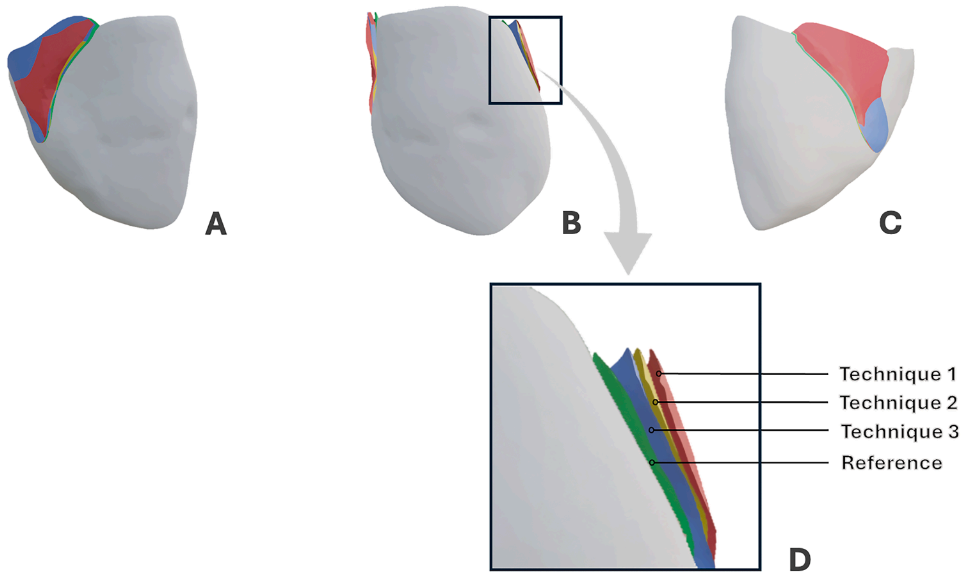


**Fig 3.** Isolation of mesial and distal interproximal surfaces. Example of the maxillary right canine. After a Boolean operation, the mesial and distal interproximal surfaces (*colored*) were isolated after superimposition of the segmented tooth models from techniques 1, 2, and 3 over the reference model. Mesial **(A)**, buccal **(B)**, and distal **(C)** aspects of the superimposed models are shown with the separated interproximal surfaces. Zoomed-in view **(D)** of the boxed area in part **B** illustrating the interproximal overlap of the 3 segmentation techniques (color-coded) relative to the reference model. The mesial and distal interproximal surfaces were subsequently cropped from each of the 4 tooth models to generate identical surfaces for superimposition and 3D deviation analysis between the reference interproximal surface and the interproximal surfaces from each of the 3 techniques.

for the presence of modeling wax in the 2 mm separating the cementoenamel junction from the bone model, an area of 2 mm around the crown was selected for orientation purposes (Fig 4, *A*). Following the determination of a reference interproximal surface (Fig 4, *B*), the surface deviation as well as the topographical characteristics of this surface for each of the three techniques, IOS alone (Fig 4, *C*), fused (Fig 4, *D*), and fused-adjusted (Fig 4, *E*), is illustrated.

### Statistical analysis

The collected data were analyzed using SPSS version 30.0 software (IBM Corp., Armonk, NY). For descriptive statistics, mean ± standard deviation (SD) was used. Data distribution was summarized graphically using box plots. Normality of the RMS distribution was verified by the Shapiro-Wilk test and homogeneity of variances using the Levene test. For parametric tests, repeated-measures analysis of variance (ANOVA), followed by the Tukey honest significant difference tests were applied; otherwise, the Friedman test, followed by the Wilcoxon signed rank test were used. The significance level was set at 5%, *P* value [0-1] ≤0.05. Pairwise comparisons were conducted between IOS (1) and fused groups (2), between IOS (1) and fused-adjusted groups (3), and between fused (2) and fused-adjusted groups (3).

## RESULTS

Using the RMS values for the 3 segmented models, the RMS error distribution by technique was illustrated using box plots (Fig 5) for each of the evaluated surfaces: total surface, interproximal surface, and outer surface. For the interproximal surface, technique 1 presented the highest median RMS, followed by technique 2, then technique 3 (Fig 5, *A*). For the outer surface, techniques 1, 2, and 3 exhibited a comparable median RMS (Fig 5, *B*). For the total surface, technique 1 presented the highest median RMS, followed by technique 2, then technique 3 (Fig 5, *C*).

The results of the statistical tests are shown in Table 1. The test results and descriptive statistics for the interproximal, outer, and total surfaces are presented sequentially below. Note that technique 1 refers to IOS segmentation alone, technique 2 involves the automated merging of IOS crowns and CBCT roots, and technique 3 involves the manual adjustment of interproximal surfaces after automated merging.

For the interproximal surface, technique 3 presented the lowest mean RMS, followed by technique 2, then

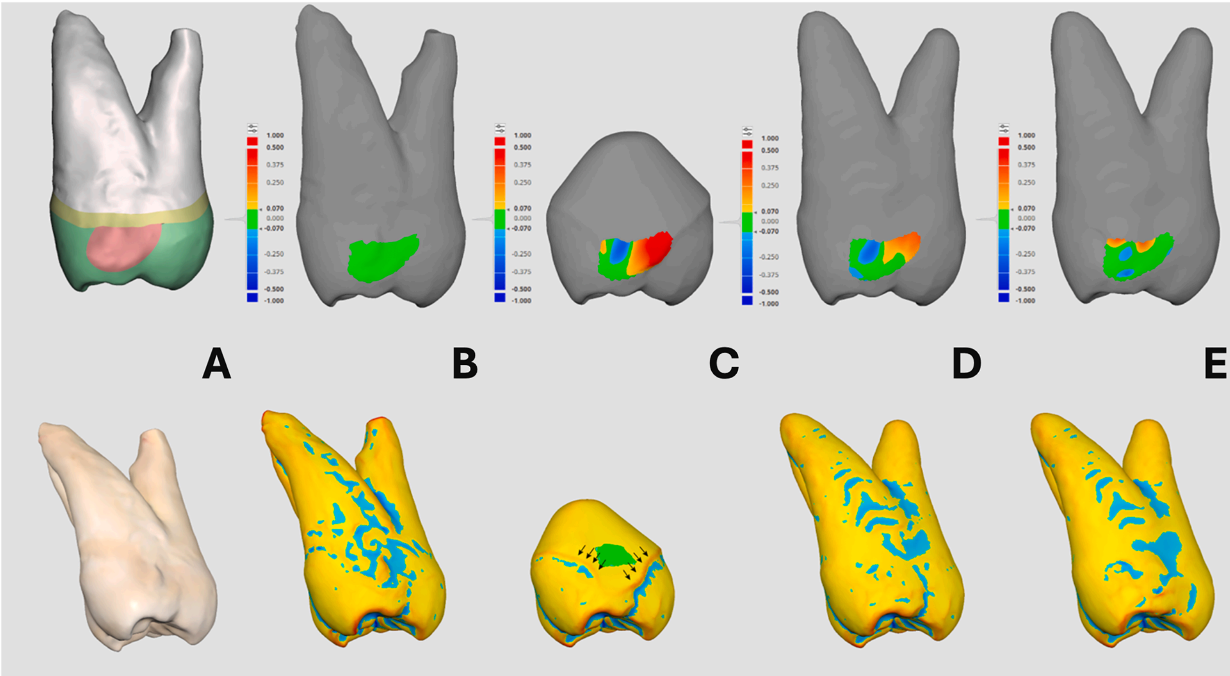


**Fig 4.** Surface deviation (*top*) and topographical analysis (*bottom*): **A,** The reference model is divided into regions of interest for subsequent deviation analysis (*pink*, interproximal surface; *green*, outer surface; *yellow*, the 2-mm bone-to-cementoenamel junction area) and taken as is for topographical analysis; **B,** Reference control model showing the isolated interproximal surface for comparison among the 3 segmentation techniques (*top*) and reference topography model (*bottom*); **C,** IOS crowns showing the least accuracy of interproximal segmentation between the groups (color bars are included for reference). The curvature display demonstrates the lack of depressions and grooves for the interproximal surface after IOS segmentation (*red*, embossed region; *blue*, engraved region; *green*, zero curvature, meaning a flat surface; *arrow*, the red boundary between the zones with rich topographical information and the rather flat interproximal surface [*green*]); **D,** Fused group showing lower deviation values and variable texture at the level of the interproximal area; **E,** Fused-adjusted model demonstrating lower deviation values (*green*) than the previous 2 models. Similar to the fused models, more topographical information is visible at the level of the interproximal area.

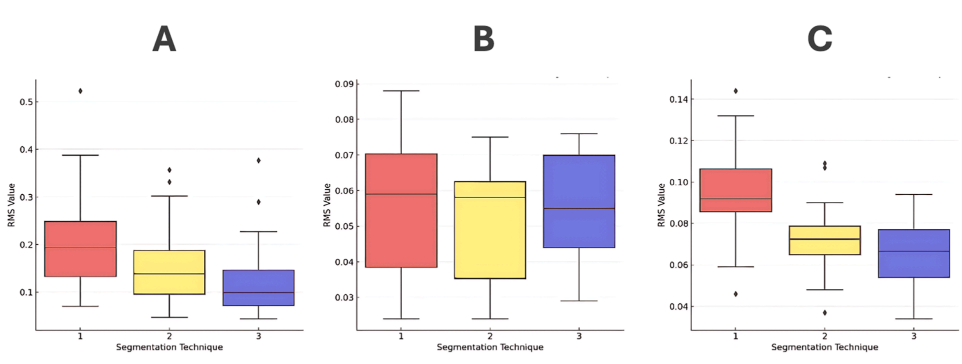


**Fig 5.** RMS error distribution by segmentation technique for the interproximal **(A)**, outer **(B)**, and total **(C)** tooth surfaces. Box-and-whisker plots illustrate the trueness values obtained with the 3 techniques: technique 1 – IOS segmentation alone, technique 2 – automated IOS–CBCT fusion, and technique 3 – manual adjustment of interproximal surfaces after automated fusion.

**Table I.** Comparison of the mean RMS values according to the region of interest of the 3 segmentation techniques

| *Surface* | *Technique* | *Mean RMS* | *Global P* | *Pairwise comparison* | *Post-hoc P* |
|---|---|---|---|---|---|
| Interproximal (n = 26) | 1 | 0.210 ± 0.151 | $7.45 \times 10^{-6}$* | 1 vs 2 | $8.16 \times 10^{-5}$* |
| | 2 | 0.159 ± 0.129 | | 1 vs 3 | $2.09 \times 10^{-6}$* |
| | 3 | 0.123 ± 0.101 | | 2 vs 3 | $1.09 \times 10^{-4}$* |
| Outer (n = 14) | 1 | 0.057 ± 0.054 | 0.718 | | |
| | 2 | 0.052 ± 0.049 | | | |
| | 3 | 0.055 ± 0.054 | | | |
| Total (n = 14) | 1 | 0.094 ± 0.089 | 0.004* | 1 vs 2 | 0.04* |
| | 2 | 0.073 ± 0.069 | | 1 vs 3 | 0.004* |
| | 3 | 0.065 ± 0.063 | | 2 vs 3 | 0.663 |

Note. Technique 1 refers to IOS alone, technique 2 refers to AI-based IOS + CBCT fusion, and technique 3 refers to AI-based IOS + CBCT fusion with manual interproximal adjustment.
Values are presented as mean RMS error ± SD.
*Statistically significant difference $P < 0.05$.

technique 1. The Friedman test indicated a statistically significant difference in RMS values among the IOS, fused, and fused-adjusted tooth models for the interproximal surface ($P < 0.05$). The Wilcoxon signed rank tests indicated a significant difference between groups 1 and 3 (lowest $P$ value), 1 and 2 ($P < 0.05$), and 2 and 3 ($P < 0.05$).

For the outer surface, repeated-measures ANOVA indicated an absence of significant difference between the segmentation techniques ($P < 0.05$).

For the total surface, the repeated-measures ANOVA test yielded a statistically significant difference among the 3 models for the total surface ($P = 0.004$). The results of the pairwise test indicated that there is a significant difference ($P = 0.04$) between the IOS segmentation alone and the fused IOS-CBCT segmented tooth models. The same was concluded between technique 1 and technique 3 ($P = 0.004$). However, no significant difference ($P = 0.663$) existed between the fused and fused-adjusted models. Thus, technique 3 did not exhibit a significantly lower mean RMS than technique 2 for the total surface.

Given the statistically significant difference among the 3 techniques for the interproximal surface, further investigation was done to determine whether there is an overestimation or an underestimation of the tooth contours at the level of the interproximal surface among the 3 segmented models compared with the reference scan. Table II presents the results of these investigations. Concerning the interproximal surface parameters, technique 1 produced larger models on average (avg = 0.097). In other words, teeth were, on average, volumetrically overestimated after segmentation at the level of the interproximal surface, resulting in a segmented tooth model that is larger mesiodistally. Technique 2 showed no consistent tendency to produce either a larger or smaller tooth model compared with the reference scan (avg = –0.002). Similarly, the relative positive bias of technique 3 was negligible (avg = 0.016). Analyzing the variability indicates that technique 1 has the lowest consistency (SD = 0.151), whereas technique 3 exhibits the lowest variability and therefore the highest consistency (SD = 0.101). A lower absolute deviation for technique 3 (abs avg = 0.087) and technique 2 (abs avg = 0.088) was found compared with technique 1, which exhibited more pronounced overall errors (abs avg = 0.138).

**Table II.** Comparison of descriptive statistics for the 3 techniques at the level of the interproximal surface

| | *Properties – interproximal surface* | | | | |
|---|---|---|---|---|---|
| *Technique* | *Avg* | *Abs avg* | *SD* | *Avg +* | *Avg –* |
| 1 | 0.097 | 0.138 | 0.151 | 0.123 | –0.086 |
| 2 | –0.002 | 0.088 | 0.129 | 0.073 | –0.083 |
| 3 | 0.016 | 0.087 | 0.101 | 0.068 | –0.063 |

## DISCUSSION

The primary objective of the study was to evaluate the interproximal surface accuracy of IOS segmented models with or without fusion of CBCT tooth roots. CBCT integration may improve AI-based interproximal reconstructions either by providing more comprehensive information on tooth axis and position for enhanced automatic feature extraction, as seen in technique 2, or by the ability to manually modify the interproximal area of surface-scanned models using volumetric information, as done in technique 3. For that reason, 2 methods of CBCT integration were included, with or without manual adjustment, to better understand these mechanisms. The easily scanned outer surfaces were chosen as a control, which was confirmed by the lack of significant difference among the segmented models for the outer surface.

The study was conducted in vitro to ensure complete scanning of extracted teeth for accurate reference models. However, the reference scan cannot be considered absolutely accurate because of the limitations inherent to intraoral scanning. The same IOS was used for both model and reference scans to ensure methodological consistency and replicate clinical conditions, in which stitching errors and other limiting factors are necessarily present. The reference scan was therefore acquired under comparable conditions, with the primary concern being adequate access to the interproximal surfaces.

Regarding the study model, several additional limitations can also be noted. For intraoral scans, in vivo factors, such as the presence of saliva and debris, undercuts the access, which is hindered by the scanner's limited freedom of movement and affects the accuracy of the resulting scan and subsequent segmentation, respectively.[4] Furthermore, CBCT scans are affected by factors, such as motion-related artefacts and variations in contrast of dental and periodontal tissues that are often absent in laboratory studies.[20] Finally, the alveolar bone model made from resin does not mimic the exact properties of alveolar bone, which may affect CBCT attenuation and segmentation performance in vivo. Although the light body impression material did achieve a similar radio-opacity to bone, the variable density of actual alveolar bone was not reproduced.

The Relu platform (Relu BV) presents a validated, fully automatic solution for IOS and CBCT tooth segmentation using advanced AI-algorithms.[21,22] The prospect of having a rapid solution to difficult segmentation tasks is promising, but further research on the software is warranted to ensure its ability to manage interproximal segmentation errors.

Importantly, this novel approach to interproximal surface reconstruction must be thoroughly validated to justify clinical applications. The present study included a single full-arch model, with a sample size of only 14 teeth. Multiple models with teeth of varying anatomy must be used to ensure that the interproximal adjustment significantly improves surface accuracy across all models. Furthermore, the absence of multiple operators raises 2 concerns. The first is that interoperator variability is not assessed, and therefore, the reproducibility of the manual adjustment is not evaluated. The second is that a single operator may raise concerns of information leakage, whereby the interproximal adjustment was done according to information from the 2 previously applied techniques. Future studies must evaluate interproximal surface accuracy using a larger sample size with multiple models, as well as multiple operators who are not exposed to previous steps. Finally, the precision of the techniques should also be evaluated using repeated scans and segmentations, as well as multiple iterations of the manual interproximal adjustment.

For the deviation analysis step, we presented a novel method for delineating the interproximal area objectively using the open crowns provided by the intraoral scan during the segmentation procedure. During AI-based IOS tooth segmentation, Relu (Relu BV) generates the closed crown by reconstructing missing crown surfaces through surface completion. Local geometric interpolation is performed using a convolutional neural network trained on a database of over 45,000 teeth. The resulting segmented IOS crown represented the algorithm's best estimate of the missing interproximal surface. Because our deviation analysis isolated the interproximal area from the closed crown, we were able to evaluate this estimate against the actual interproximal surface. There is an absence in the literature of a method for evaluating specific surfaces of a tooth during tooth segmentation, with studies such as that of Yacout et al[11] and Im et al[15] using mesiodistal widths and overall surface deviations to evaluate segmentation accuracy. Furthermore, Baldini et al[21] and Wang et al[22] evaluated the accuracy of fusion models at the level of individual teeth, without considering any discrepancies that might exist among tooth surfaces. Therefore, the study is unique in its objectives because little information exists on the comparative reproduction of the interproximal surface using different segmentation techniques.

Because there was a need to evaluate the interproximal surface on its own, a decision had to be made between isolating the surface or selecting it without separating it from the overall tooth model. The preliminary study done for the present project revealed that different values of RMS were given based on the technique of comparison used, which could be due to the excess surfaces around the interproximal surface that affect the stability of the RMS value. This finding led us to adopt a method similar in the literature to that of Triduo et al,[23] in which a specific region of interproximal reduction was isolated from the total tooth model. Furthermore, Eid et al[24] used Medit Design, derived from the Medit Link software (Medit), to conduct deviation analysis after the superimposition of tooth models, which corroborates our decision to use the same software for that purpose. Using Medit Link (Medit) was also proposed by Yilmaz et al[25] to measure surface deviations.

A significant difference for the interproximal surface was found among the 3 models, and the most accurate interproximal reconstruction was obtained with manual refinement. However, for the total crown surface, significant differences were found between IOS and fused models from techniques 2 and 3, but not between fused models themselves. This is in agreement with the findings of Jang et al,[26] who found that the fusion method was more accurate than IOS alone because it eliminates any stitching errors from preliminary IOS. Furthermore, Liu et al[27] found that fused models are more accurate than single-modality IOS or CBCT-segmented models. However, it is important to note that although there was no difference between techniques 2 and 3 in terms of total surface, mesiodistal widths are taken only at 2 specific points of the tooth, and any segmentation error at this level may be overlooked by total surface comparisons. Therefore, the difference in interproximal surface accuracy between techniques 2 and 3 may still be significant if the mesiodistal tooth widths were taken after tooth segmentation. Preda et al[28] considered that there is no need to manually adjust the segmented fused models because they are sufficiently accurate. However, as our results demonstrate, insufficient interproximal accuracy may remain unobserved if surface-based analysis is not conducted. To illustrate this finding, the $P$ value for comparisons between techniques 2 and 3 for the total surface was 0.663. For the interproximal surface, it became significantly less than 0.05. Furthermore, the mean RMS for the total surface was 0.073 with technique 2 and 0.065 with technique 3, which then increased at the level of the interproximal surface to 0.159 and 0.123, respectively. This demonstrates the potential added value of manual adjustment using CBCT scans on interproximal surface accuracy. To further support this, not only did techniques 2 and 3 significantly differ for the interproximal surface, but also AI-based IOS-CBCT fusion exhibited a more accurate reproduction of the interproximal area. D'Alessandro et al[29] suggested that CBCT-IOS fusion is useful for root movement monitoring in orthodontic treatment plans. However, our findings suggest an additional advantage for multimodal fusion in enhancing tooth segmentation accuracy in difficult areas. Finally, a possible explanation for the superiority of automatic fusion methods compared with IOS alone, although the IOS crown is used in both methods, is the self-corrective nature of AI algorithms, because of factors such as global context[30] and emergent properties.[31] Therefore, the present study elucidates a potential superior accuracy of fusion methods compared with IOS alone because of the ability of manual refinement of the interproximal area (technique 3), as well as the richness of the information provided by different modalities on the crown surface and position (technique 2).

In our study, the IOS-segmented models produced larger models on average compared with the reference model (avg = 0.097), which agrees with the findings of Yacout et al[11] and Woo et al,[32] in which automatic tooth segmentation from Medit Orthosimulation software (Medit) also overestimated the mesiodistal widths of the teeth. The overestimation of tooth size by IOS models would have adverse effects on the ability to provide accurate treatment predictions, as discussed by Yacout et al,[11] Baumgaertel et al,[33] and Sherrard et al,[34] who determined that mesiodistal widths were underestimated when evaluated on CBCT scans. On the other hand, IOS-CBCT fused models did not exhibit a tendency to underestimate or overestimate the actual size of the teeth after tooth segmentation (avg = −0.002). The replacement of CBCT crowns with IOS crowns, the smoothening done at the junction of CBCT roots and IOS crowns, and the novel algorithms used for automatic CBCT and IOS tooth segmentation may have contributed to the improvement in reproducing accurate tooth dimensions after segmentation. Similarly, technique 3 exhibited a slight tendency to overestimate tooth size (avg = 0.016). The dimensions of teeth, especially at the level of interdental contacts, must be accurate, given their impact on clinical outcomes, such as interproximal reduction predictions and treatment planning in clear aligner therapy (CAT). Yacout et al[11] obtained a discrepancy of 0.2 mm in the mesiodistal tooth dimensions after IOS tooth segmentation, which is significant in CAT because teeth are moved one-tenth of a mm with each tray. Therefore, further investigations on the quantitative impact of failed interproximal surface reconstruction are warranted. The discrepancy with technique 3 may be related to the nonstandardized adjustment, with no evaluation of interoperator variability.

## CONCLUSIONS

This preliminary study introduced a method of improving interproximal reconstructions using combined crown-root models. Within the limitations of the present study, the following can be concluded:

1. The interproximal surface inaccuracies were primarily responsible for statistically significant differences observed among the 3 models.
2. The AI IOS-CBCT fusion itself provided more accurate tooth models overall compared with IOS crowns alone, as demonstrated by method-based analysis.
3. Manual interproximal adjustment of fused models significantly improved the interproximal surface accuracy, as demonstrated by surface-based analysis.
4. In addition to root monitoring capabilities, another benefit of CBCT integration in CAT, related to improved segmentation accuracy, was proposed.

The implications of these results on digital diagnosis, treatment planning, and appliance design must be evaluated in the clinical setting to determine the true bearing of an optimal segmentation accuracy at the level of the interproximal surfaces.

## AUTHOR CREDIT STATEMENT

Amir Salloum contributed to conceptualization, writing–original draft, investigation, data analysis, and interpretation of data; Nabil Ghosn contributed to methodology, data curation, figures and illustrations, data analysis, and writing–original draft; Alain Tauk contributed to writing–review and editing; Roland Kmeid contributed to writing–review and editing; and Joseph Bou Serhal contributed to supervision and project administration.

## DECLARATION OF AI AND AI-ASSISTED TECHNOLOGIES IN THE WRITING PROCESS

During the preparation of this work, the authors used the GPT-5.2 model from ChatGPT (OpenAI, San Francisco, CA, USA) to generate color-coded box plots. After using this service, the authors reviewed and edited the content as needed in conversation with a statistician and take full responsibility for the content of the publication.

## SUPPLEMENTARY DATA

Supplementary data associated with this article can be found, in the online version, at https://doi.org/10.1016/j.ajodo.2025.11.025.

## REFERENCES

1. Trelenberg-Stoll V, Drescher D, Wolf M, Becker K. Automated tooth segmentation as an innovative tool to assess 3D-tooth movement and root resorption in rodents. Head Face Med 2021;17:3.
2. Adnan N, Khalid WB, Umer F. An artificial intelligence model for teeth segmentation and numbering on orthopantomograms. Int J Comput Dent 2023;26:301-9.
3. Elgarba BM, Van Aelst S, Swaity A, Morgan N, Shujaat S, Jacobs R. Deep learning-based segmentation of dental implants on cone-beam computed tomography images: a validation study. J Dent 2023;137:104639.
4. Alkadi L. A comprehensive review of factors that influence the accuracy of intraoral scanners. Diagnostics (Basel) 2023;13:3291.
5. Nedelcu R, Olsson P, Nyström I, Rydén J, Thor A. Accuracy and precision of 3 intraoral scanners and accuracy of conventional impressions: a novel in vivo analysis method. J Dent 2018;69:110-8.
6. Al-Ubaydi AS, Al-Groosh D. The validity and reliability of automatic tooth segmentation generated using artificial intelligence. ScientificWorldJournal 2023;2023:5933003.
7. Winkler J, Gkantidis N. Trueness and precision of intraoral scanners in the maxillary dental arch: an in vivo analysis. Sci Rep 2020;10:1172.
8. Qian J, Lu S, Gao Y, Tao Y, Lin J, Lin H. An automatic tooth reconstruction method based on multimodal data. J Vis 2021;24:205-21.
9. Son SA, Kim JH, Seo DG, Park JK. Influence of different inlay configurations and distance from the adjacent tooth on the accuracy of an intraoral scan. J Prosthet Dent 2022;128:680-7.
10. Im J, Cha JY, Lee KJ, Yu HS, Hwang CJ. Comparison of virtual and manual tooth setups with digital and plaster models in extraction cases. Am J Orthod Dentofacial Orthop 2014;145:434-42.
11. Yacout YM, Eid FY, Tageldin MA, Kassem HE. Evaluation of the accuracy of automated tooth segmentation of intraoral scans using artificial intelligence-based software packages. Am J Orthod Dentofacial Orthop 2024;166:282-91.e1.
12. Vinayahalingam S, Kempers S, Schoep J, Hsu TH, Moin DA, van Ginneken B, et al. Intra-oral scan segmentation using deep learning. BMC Oral Health 2023;23:643.
13. Kubík T, Španěl M. LMVSegRNN and Poseidon3D: addressing challenging teeth segmentation cases in 3D dental surface orthodontic scans. Bioengineering (Basel) 2024;11:1014.
14. Chen X, Ma N, Xu T, Xu C. Deep learning-based tooth segmentation methods in medical imaging: a review. Proc Inst Mech Eng H 2024;238:115-31.
15. Im J, Kim JY, Yu HS, Lee KJ, Choi SH, Kim JH, et al. Accuracy and efficiency of automatic tooth segmentation in digital dental models using deep learning. Sci Rep 2022;12:9429.
16. Kim T, Cho Y, Kim D, Chang M, Kim YJ. Tooth segmentation of 3D scan data using generative adversarial networks. Appl Sci 2020;10:490.
17. Li J, Cheng B, Niu N, Gao G, Ying S, Shi J, et al. A fine-grained orthodontics segmentation model for 3D intraoral scan data. Comput Biol Med 2024;168:107821.
18. International Organization for Standardization. Accuracy (trueness and precision) of measurement methods and results— part 1: basic provisions and definitions (ISO 5725-1:2023). Available at: https://www.iso.org/obp/ui/#iso:std:iso:5725:-1:ed-2:v1:en. Accessed June 25, 2025.
19. Dghaily D, Rayyan M, Ragab H, Sayed M, Ayash G, Alzahrani G. Comparison of fracture resistance between different treatment modalities of mutilated endodontically treated teeth using polyether ether ketone. J Contemp Dent Pract 2023;24:668-73.
20. Ali AS, Sarti C, Landi C, Fusiello A. Motion compensation in short-scan CBCT reconstructions for dental applications. Image Process 2024;12926:394-402.
21. Baldini B, Papasratorn D, Fagundes FB, Fontenele RC, Jacobs R. Validation of a novel tool for automated tooth modelling by fusion of CBCT-derived roots with the respective IOS-derived crowns. J Dent 2025;153:105546.
22. Wang X, Alqahtani KA, Van den Bogaert T, Shujaat S, Jacobs R, Shaheen E. Convolutional neural network for automated tooth segmentation on intraoral scans. BMC Oral Health 2024;24:804.
23. Triduo M, Zubizarreta-Macho Á, Pérez-Barquero JA, Guinot Barona C, Alvarado Lorenzo A, Vicente-Galindo P, et al. A novel digital technique to quantify the area and volume of enamel removal after interproximal enamel reduction. Appl Sci 2021;11:1274.
24. Eid FY, Sabouni W, Zaher A, Tageldin MA, Elfouly D. Comparison of three-dimensional tooth movements in virtual setups using different software packages for clear aligner therapy. BMC Oral Health 2025;25:549.
25. Yilmaz B, Marques VR, Donmez MB, Cuellar AR, Lu WE, Abou-Ayash S, et al. Influence of 3D analysis software on measured deviations of CAD-CAM resin crowns from virtual design file: an in-vitro study. J Dent 2022;118:103933.
26. Jang TJ, Yun HS, Hyun CM, Kim JE, Lee SH, Seo JK. Fully automatic integration of dental CBCT images and full-arch intraoral impressions with stitching error correction via individual tooth segmentation and identification. Med Image Anal 2024;93:103096.
27. Liu J, Hao J, Lin H, Pan W, Yang J, Feng Y, et al. Deep learning-enabled 3D multimodal fusion of cone-beam CT and intraoral mesh scans for clinically applicable tooth-bone reconstruction. Patterns (N Y) 2023;4:100825.

28. Preda F, Nogueira-Reis F, Stanciu EM, Smolders A, Jacobs R, Shaheen E. Validation of automated registration of intraoral scan onto cone beam computed tomography for an efficient digital dental workflow. J Dent 2024;149:105282.
29. D'Alessandro AC, D'Antò V, Razionale AV, Allesandri-Bonetti G. Integrating CBCT and virtual models for root movement with clear aligners. J Clin Orthod 2020;54:159-66.
30. Wu Y, Yan H, Ding K. Transformer based 3D tooth segmentation via point cloud region partition. Sci Rep 2024;14:28513.
31. Hamilton A. Artificial intelligence and healthcare simulation: the shifting landscape of medical education. Cureus 2024;16:e59747.
32. Woo H, Jha N, Kim YJ, Sung SJ. Evaluating the accuracy of automated orthodontic digital setup models. Semin Orthod 2023;29:60-7.
33. Baumgaertel S, Palomo JM, Palomo L, Hans MG. Reliability and accuracy of cone-beam computed tomography dental measurements. Am J Orthod Dentofacial Orthop 2009;136:19-25.
34. Sherrard JF, Rossouw PE, Benson BW, Carrillo R, Buschang PH. Accuracy and reliability of tooth and root lengths measured on cone-beam computed tomographs. Am J Orthod Dentofacial Orthop 2010;137:S100-8.